Solution to the bistability problem in shear force distance regulation encountered in scanning force and near-field optical microscopes

A. V. Zvyagin, J. D. White,[a] M. Kourogi, M. Kozuma, and M. Ohtsu
Tokyo Institute of Technology, Nagatsuta 4259, Yokohama 227, Japan

(Received 31 March 1997; accepted for publication 27 August 1997)

The bistability problem, common to scanning microscopes employing lateral dithering of the probe for image formation (i.e., shear force microscope) or probe-sample distance control (i.e., near-field optical microscope) is shown to stem from the two nearly degenerate vibration degrees of freedom possessed by a laterally dithered fiber. Controlling the fiber vibration direction by means of a four-sectioned piezo was found to be a simple and effective solution of the problem. An image of a microtubule is presented to demonstrate the improved imaging ability. © *1997 American Institute of Physics.* [S0003-6951(97)03843-6]

The shear force and near-field optical microscopes (NOMs) are members of the family of scanning probe microscopes. The former is a type of noncontact scanning force microscope (SFM)[1] [the atomic force microscope (AFM) is a type of contact SFM] distinguished by its use of shear force to map the topographic surface of a sample. It is especially desirable for biological samples, because it exerts far less force on the sample than the competing AFM techniques. The latter exploits the spatial localization[2] of the optical near-field in order to achieve subwavelength resolution without harming a sample. In many NOM systems shear force control is used to keep the nanometric sized probe close to the sample surface.

This letter will discuss the origin of the problem of bistability in the shear force feedback signal, present a simple solution and its incorporation in a mechanically and thermally stable system, and illustrate the improved resolution with a topographic image[3] of a soft (i.e., low mechanical compliance) biological sample (microtubule).

Shear force control of probe-sample separation is implemented as follows: A sharpened fiber tip is glued on a piezoelectric transducer (PZT). For shear force purposes, it has one fixed and one free end and fiber is vibrated laterally by applying a dithering voltage to the PZT at a frequency close to a fiber eigenfrequency [Fig. 1(a)]. (A typical 1.5-mm-long, $\phi 40\ \mu$m glass fiber has its first harmonic resonance at 20 kHz with a quality factor of 200). When the fiber comes within ~10 nm [c.f. Fig. 1(b)] of a surface, the tip enters the range of attractive Van der Waals and/or capillary forces, $\mathbf{F}_w$,[1] which are a function of the probe-sample separation. The component of this force perpendicular to the fiber axis $\mathbf{F}_r \cong -|\mathbf{F}_w|\varphi \mathbf{e}_\varphi$ acts to oppose the motion of the fiber, causing a shift of the fiber's resonance to higher frequency and an accompanying reduction of the amplitude of the tip vibration. This tip vibration can be detected by a variety of methods,[4–8] among which the stray light detection method[9–11] has proved to be simple, robust, and sensitive. As described in Fig. 1(a), a laser beam is focused onto the fiber tip, and the diffracted light detected by a photodiode. This signal, containing information on the tip vibration frequency and amplitude, is heterodyned with the dithering frequency applied to the fiber. At a great distance from the surface the fiber's vibration frequency is equal to the applied dithering frequency; close to the surface the change in the fiber's resonance frequency results in a sharp drop in lock-in amplifier output. A proportional integration controller compares the lock-in output with a preset value and feeds back the difference to a Z-positioning piezo, thus keeping the tip at a predetermined height above the sample. This works provided

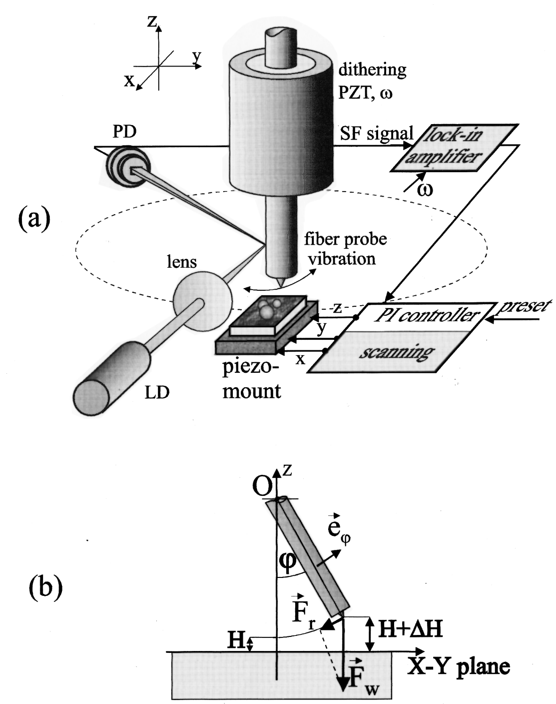

FIG. 1. Explanation of the shear force probe-sample separation regulation as employed in a shear force or near-field optical microscope. (a) LD represents a laser diode ($\lambda = 1.3\ \mu$m wavelength in our case) and PD a photodiode. The fiber probe is dithered at its near resonant frequency, ω, by means of a voltage applied to the PZT. (b) Force diagram of a fiber coupled to the surface. The XY plane coincides with the sample plane, Z is the fiber vibration axis in the direction perpendicular to the sample surface, $\mathbf{e}_\varphi$ is angular unit vector defined in the plane where the fiber vibration takes place, φ is total displacement angle, $\mathbf{F}_w$ is Van der Waals and capillary attractive forces, $\mathbf{F}_r$ is restoring force, H is altitude of the fiber tip, $\delta H = o(\varphi^2)$, and therefore is neglected.

[a]Kanagawa Academy of Science and Technology, Kawasaki 213, Japan. Electronic mail: whitejd@net.ksp.or.jp

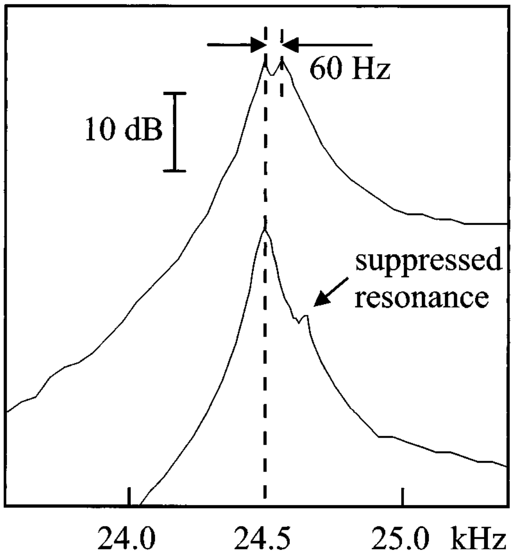

FIG. 2. Frequency spectrum of the fiber under lateral dithering. The two resonance peaks are separated by ~60 Hz. The network analyzer resolution bandwidth=10 Hz. In the upper trace the amplitude of the two resonant peaks are equal, while in lower trace the high frequency peak has been suppressed by greater than 10 dB using the scheme illustrated in Fig. 3.

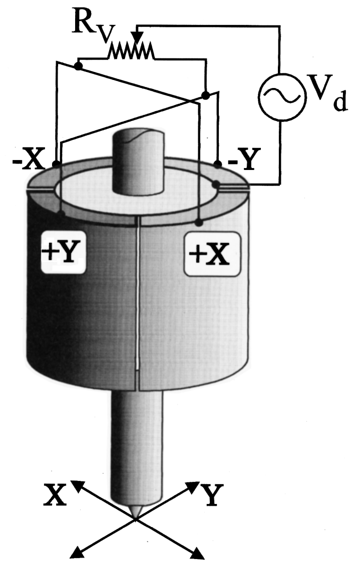

FIG. 3. Schematic diagram of the fiber lateral vibration direction regulation for the suppression of one fiber resonance. The fiber is attached to a four-sectioned piezo tube to which a dithering voltage V_d is applied. $+X$ denotes the PZT segment which shrinks upon applying positive voltage between outer and inner common electrode, while $-X$ denotes the expanding segment. Y is similarily denoted.

the dependence of the sample-probe separation on the vibration amplitude is monotonic.[4]

Unfortunately, the dependence of the sample-probe separation on the vibration amplitude is not necessarily monotonic, due to the two degrees of freedom possessed by a laterally vibrated fiber. Let us consider the vibrating system in a coordinate system [defined in Fig. 1(b)] in which the origin, O, is placed at the fiber clamping point. The motion of the fiber's tip thus takes place equidistantly with respect to the origin, and can be analytically described by a two-dimensional vector $\boldsymbol{\varphi}=\varphi\mathbf{e}_\varphi=\varphi_x\mathbf{e}_x+\varphi_y\mathbf{e}_y$ with $\mathbf{e}_x,\mathbf{e}_y$ being the elementary orthogonal angle unit vectors in the XOZ and YOZ planes, respectively; φ_x, φ_y are the fiber deflection angle projections onto the XOZ (YOZ) plane. The fiber tip motion is governed by a set of differential equations:

$$\begin{cases} \ddot{\varphi}_x+2\gamma\dot{\varphi}_x+(\omega_{0x}+\Delta\omega_w)^2\varphi_x=f_x\cos\omega t \\ \ddot{\varphi}_y+2\gamma\dot{\varphi}_y+(\omega_{0y}+\Delta\omega_w)^2\varphi_y=f_y\cos\omega t \end{cases}, \tag{1}$$

where γ is a damping constant of the fiber tip; $\omega_{0x}(\omega_{0y})$ is eigenfrequency of the fiber tip along the $x(y)$ axis; $\Delta\omega_w \equiv\Delta\omega_w(H)$ is the separation dependent frequency shift in the fiber tip's eigenfrequency due to coupling the fiber to the surface through Van der Waals and/or capillary forces; ω is the applied dithering angular frequency (near the fiber's resonant frequency); and $f_x(f_y)$ is the vibration amplitude along the $x(y)$ axis of the fiber dithering. This equation is only of a representative order of magnitude due to the complicated structure of forces involved in the probe–sample interaction. Ideally these two lateral vibrations are degenerate ($\omega_{0x}=\omega_{0y}$). Unfortunately, due to uncontrolled factors, such as oblique fiber attachment to the dithering piezo and/or slight asymmetries in the fiber probe itself, this degeneracy is removed. Figure 2 (upper trace) shows a double resonance structure in which the two peaks are separated by 60 Hz. To illustrate the serious consequences of this doublet structure for shear force control, let us consider a fiber being dithered at the higher frequency resonance. When it enters the attractive force range, along with a fall in vibration amplitude, the fiber's resonance frequency shifts in the positive direction as it is no longer a ''free end'' [c.f. Eq. (1)], and hence the dithering frequency ω applied to the fiber is no longer at a fiber's resonance. By the time the amplitude has dropped to half of its original magnitude, due to the surface-probe interaction, the fiber's resonance frequency has shifted by $\omega/2Q=+2\pi\times 60$ rad/s as a simple estimation based on Eq. (1) shows. The applied dither is now resonant to the lower frequency resonance. This results in severe oscillations in the shear force servo system. As these two peaks often lie very close together, this doublet structure may not be recognized when choosing a frequency to dither the fiber (due to inadequate resolution of the spectrum analyzer being used to find the peaks), only showing itself in the form of unexplained system instabilities. Among a variety of empirical methods to obtain a stable shear force signal, we are aware of the following: trying successive harmonics of the fiber resonance frequency until one giving a stable approach curve is found; choosing an off-resonance frequency on which to vibrate the fiber; or when two peaks were seen, operating on the lower frequency peak.[12] The first two techniques are quite time consuming and although the third technique, dithering the fiber at the lower frequency peak, is to be preferred over vibrating at the higher frequency peak it cannot halt servo loop oscillations caused by external perturbations or/and sample topography.

We have succeeded in removing this doublet structure simply and effectively by using a four-sectioned dithering piezo (shown schematically in Fig. 3). The dithering voltage is distributed by means of a variable resistor (R_v). By varying the value of R_v from 0 to its maximum value one can gradually switch the fiber vibration from along the y axis to

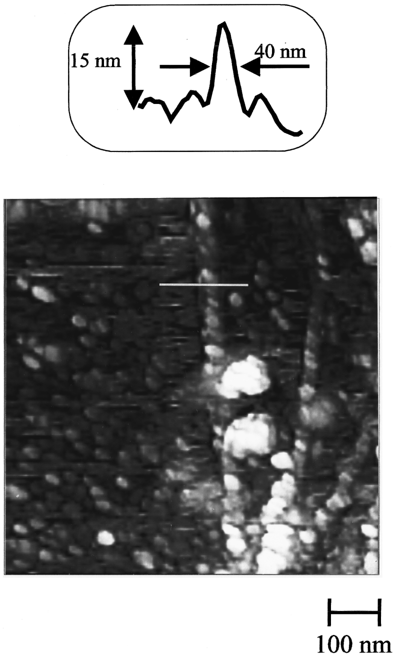

FIG. 4. Shear force image of protein stabilized microtubules. Three filaments spread radially from the right bottom corner of the image. The bright round structures also visible in this image are protein aggregates. The top inset shows profile of a microtubule taken along the line marked in the main figure.

along the x axis. This allows either of the two fiber resonances to be suppressed or enhanced. Figure 2 demonstrates the suppression of an undesirable high frequency peak by 10 dB by adjusting the variable resistor. This allows stable operation of the shear force servo loop in the middle of the force curve (where it is the steepest and thus most sensitive).

This improved shear force detection system has been incorporated into a highly compact and stable combination shear force, collection-mode NOM. The kinematic part of the setup consists of two coaxial piezo tubes. The outer tube supports a wagon on which the prism and sample are mounted and is used for both lateral scanning and fine vertical positioning. In addition, it operates as a motor for the vertical piezoelectric inertial slider[13] used for coarse vertical positioning. During scanning, the servo loop Z voltage as well as the X-Y scanning voltage are applied to the outer PZT. The inner tube holds and dithers the gold coated sharpened optical fiber. The topographic shear force image is created by recording the shear force feedback signal, and the optical NOM image by recording the intensity of light transmitted through the fiber as it is scanned laterally across the surface of the sample. All components were mounted on an invar plate, placed on a damping stage.

To confirm the improved imaging resolution obtained by eliminating this bistability, Fig. 4 presents a topographic image of a soft biological specimen (microtubule with associated proteins) chosen for its well identified nanometric size (25–30 nm in diameter and microns in length) and importance biologically. The observed width (40 nm) and height (15 nm) are in agreement with previous observations that dried and fixed microtubules take a squeezed tubular, rather than circular tubular shape,[14] and agree with NOM data obtained using this instrument.[3] To the best of our knowledge, this image exhibits the best spatial resolution of a microtubule obtained using a laterally dithered scanning force microscope.[15]

In summary, oscillations of the shear force control servo system can be caused by the nonmonotonic dependence of the tip lateral dithering amplitude on the probe-sample separation. This bistability, at least partly due to the existence of two near degenerate resonances of the fiber tip, can be removed simply by redistributing the voltage between terminals in a four-sectioned dithering PZT so as to match the applied voltage to one of the nearly degenerate modes.

[1] U. Hartmann, Adv. Electron. Electron Phys. **87**, 49 (1994).
[2] See for example, *Near-Field Optics*, edited by D. W. Pohl and D. Courjon (Kluwer Academic, Dordrecht, 1993); M. Ohtsu, J. Lightwave Tech. **13**, 1200 (1995).
[3] Optical results are presented in A. V. Zvyagin, J. D. White, and M. Ohtsu, Opt. Lett. **22**, 955 (1997).
[4] E. Betzig, P. L. Finn, and J. S. Weiner, Appl. Phys. Lett. **60**, 2484 (1992).
[5] R. Toledo-Crow, P. C. Yang, Y. Chen, and M. Vaez-Iravani, Appl. Phys. Lett. **60**, 2957 (1992).
[6] J. W. Hsu, M. Lee, and B. S. Deaver, Rev. Sci. Instrum. **66**, 3177 (1995).
[7] K. Karrei and R. D. Grober, Appl. Phys. Lett. **66**, 1842 (1995).
[8] A. Drabenstedt, J. Wrachtrup, and C. von Borczyskowski, Appl. Phys. Lett. **68**, 3497 (1996).
[9] R. D. Grober, T. D. Harris, J. K. Trautman, and E. Betzig, Rev. Sci. Instrum. **65**, 626 (1994).
[10] F. F. Froehlich and T. D. Milster, Appl. Phys. Lett. **65**, 2254 (1994).
[11] C. C. Wei, P. K. Wei, and W. Fann, Appl. Phys. Lett. **67**, 3835 (1995).
[12] W. Jhe and R. Uma Maheswari (private communications).
[13] Ch. Renner, Ph. Niedermann, A. K. Kent, and Ø. Fisher, Rev. Sci. Instrum. **61**, 965 (1990).
[14] W. Valter, W. Fritzsche, A. Schaper, K. J. Bohm, E. Unger, and T. M. Jovin, J. Cell. Sci. **108**, 1063 (1995).
[15] High resolution images of microtubules have been obtained under liquid conditions using tapping mode AFM. M. Fritz, M. Radmacher, J. P. Cleveland, M. W. Allersma, R. J. Stewart, R. Gieselmann, P. Janmey, C. F. Schmidt, and P. K. Hansma, Langmuir **11**, 3529 (1995).